Infrared Spectra of Substituted Polycyclic Aromatic Hydrocarbons

Stephen R. Langhoff,[†] Charles W. Bauschlicher, Jr.,*[,‡] Douglas M. Hudgins,[§] Scott A. Sandford,[§] and Louis J. Allamandola[§]

National Aeronautics and Space Administration Ames Research Center, Moffett Field, California 94035

Received: September 29, 1997; In Final Form: November 26, 1997

Calculations are carried out using density functional theory (DFT) to determine the harmonic frequencies and intensities of 1-methylanthracene, 9-methylanthracene, 9-cyanoanthracene, 2-aminoanthracene, acridine, and their positive ions. The theoretical data are compared with matrix-isolation spectra for these species also reported in this work. The theoretical and experimental frequencies and relative intensities for the neutral species are in generally good agreement, whereas the positive ion spectra are only in qualitative agreement. Relative to anthracene, we find that substitution of a methyl or CN for a hydrogen does not significantly affect the spectrum other than to add the characteristic methyl C−H and C≡N stretches near 2900 and 2200 cm^{-1}, respectively. However, addition of NH_2 dramatically affects the spectrum of the neutral. Not only are the NH_2 modes themselves strong, but this electron-withdrawing group induces sufficient partial charge on the ring to give the neutral molecule spectra characteristics of the anthracene cation. The sum of the absolute intensities is about four times larger for 2-aminoanthracene than those for 9-cyanoanthracene. Substituting nitrogen in the ring at the nine position (acridine) does not greatly alter the spectrum compared with anthracene.

1. Introduction

Because of the tremendous stabilization afforded by π-electron delocalization, polycyclic aromatic hydrocarbons (PAHs) are ubiquitous in our everyday surroundings. For example, they are the dominant component of coals and coal-derived liquids and are important byproducts of petroleum manufacture.[1] They also constitute a major part of the soot formed in combustion processes[2] and, as such, given their well-documented biological activity,[3] represent important environmental pollutants. In addition to their terrestrial importance, PAHs are also one of the major classes of molecular species found in the interstellar medium (ISM).[4,5]

Because of their relative importance for both terrestrial and astrophysical concerns, the spectral behavior of PAHs and PAH-related species has received extensive theoretical and experimental attention in recent years. Ab initio calculations are now available for the vibrational frequencies and intensities of a substantial number of neutral and ionized PAHs,[6−8] and extensive laboratory work has been carried out on both PAHs in the gas phase[9−11] and in matrix isolation.[12,13] The majority of this work has concentrated on simple, unfunctionalized PAHs (i.e., PAHs that contain only carbon and hydrogen arranged in fused benzenoid rings). Only recently has some theoretical and laboratory work begun to appear on the spectral properties of PAHs containing peripheral chemical side groups.[10,11,14] Nonetheless, PAHs with side groups are of great interest for both terrestrial and astrophysical issues.

It has been shown that PAHs in the terrestrial atmosphere can gain chemical side groups through a variety of processes.[15] The presence of side groups can substantially effect the biological activity of these molecules. For example, the presence of methyl side groups can either increase or decrease the tumorigenicity of a PAH depending on its location.[16] Similar effects are seen for side groups containing oxygen[1] and nitrogen.[18] Studies have also indicated that PAHs with side groups are of astrophysical importance as well. A major fraction of organic material in most meteorites is in the form of aromatic materials,[19] at least some of which have an interstellar heritage as evidenced by their large deuterium excesses.[20] PAHs have also been detected in interplanetary dust particles (IDPs) thought to come from asteroids and comets.[21,22] PAHs from both sources frequently carry functional groups. Methyl side groups are the most common, but ethyl, biphenyl, isobutyl, isopropyl, hydroxyl, and N-bearing functionalities are also seen.[22,23] PAHs with side groups may also be the carriers responsible for certain enigmatic emission bands seen in the infrared spectra of nebulae in the interstellar medium.[5,24] Recent ab initio calculations have shown[25] that some of these side groups, such as NH_2 and CN, are more strongly bound to anthracene and anthracene cation than the methyl side groups.

Given the potential importance of PAHs with side groups, and the relative paucity of relevant theoretical and laboratory data, we have undertaken a study of the mid-infrared spectra of a number of these species. In this paper we compare the results of ab initio calculations with laboratory matrix-isolation spectra for the PAHs 9-cyanoanthracene (9-anthracenecarbonitrile), 2-aminoanthracene, acridine, 1-methylanthracene, and 9-methylanthracene. These molecules are shown in Figure 1.

This paper is organized as follows. The computational details are given in section 2, and the experimental details of our studies are briefly discussed in section 3. The laboratory spectra and computational results are compared in section 4. Our results are summarized in section 5.

2. Computational Methods

We follow the approach used in our earlier study[8] of unsubstituted PAHs in that we compute the harmonic frequen-

[†] Computational Chemistry Branch, Mail Stop 230-3.
[‡] Space Technology Division, Mail Stop 230-3.
[§] Astrophysics Branch, Mail Stop 245-6.

S1089-5639(97)03156-3 CCC: $15.00
Published on Web 02/07/1998

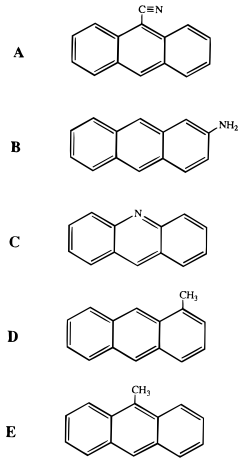

Figure 1. The molecules considered in this work: (A) 9-cyanoanthracene, (B) 2-aminoanthracene, (C) acridine, (D) 1-methylanthracene, and (E) 9-methylanthracene.

cies using the density functional theory (DFT) approach. We use the B3LYP[26] hybrid[27] functional which includes some rigorous Hartree−Fock exchange as well as including both a gradient correction for exchange and correlation. The B3LYP calculations were performed using the Gaussian 94 computer codes[28] on the Computational Chemistry IBM RISC System/6000 computers. The geometries can be obtained at http://ccf.arc.nasa.gov/∼ cbauschl/astro.geometry.

We have used the 4-31G basis set[29] throughout. Calibration calculations,[30] which have been carried out for selected unsubstituted systems, show that a single scale factor of 0.958 brings the B3LYP harmonic frequencies computed using the 4-31G basis set into excellent agreement with the experimental fundamentals; for example, in naphthalene the average absolute error is 4.4 cm^{-1} and the maximum error is 12.4 cm^{-1}. While the error can be reduced by increasing the basis set, provided the C−H stretches are scaled separately, the B3LYP/4-31G results are of sufficient accuracy to allow a critical evaluation of experiment. In addition, this basis set facilitates a comparison with our earlier work for the hydrogenated species and can be used to study larger systems. While scaling the 4-31G harmonics yields very reliable frequencies, the calibration calculations also show that the computed B3LYP/4-31G intensities are accurate except for C−H stretches, which on the average are about a factor of 2 larger than those determined in the matrix studies.[31] While the gas-phase data are very limited, it appears that the gas-phase intensities tend to lie between the matrix and B3LYP values. We also observe that when two bands of the same symmetry are close in energy, their relative intensities are sensitive to the level of theory, but that the sum of their intensities is very reliable.

As discussed previously,[30] many of the methyl PAHs are found to have lower symmetry than expected, due to a slight rotation of the methyl about the C−C bond. Relative to the higher symmetry results, this methyl rotation eliminates the imaginary frequency, but has negligible effect on the other vibrational bands. Since we believe that this effect is caused by a numerical problem, we avoid it by performing all of the calculations involving the methyl-substituted PAHs in no symmetry, even though the true symmetry may be C_s.

3. Experimental Methods

The experimental apparatus and methodology used for these matrix-isolation studies have been described in detail previously.[7,13,32] Briefly, the PAHs were codeposited onto a cold (10 K) infrared transparent window (CsI) along with a large overabundance of argon to a thickness appropriate for measurement of their infrared spectra. The window was suspended inside an ultrahigh vacuum chamber ($P \approx 10^{-8}$ mTorr), cooled by a closed-cycle helium refrigerator, and mounted so that the infrared window can be rotated to face a number of different ports without breaking vacuum.

The PAHs used in this investigation were 9-cyanoanthracene (9-anthracenecarbonitrile; Aldrich, 97% purity), 2-aminoanthracene (Aldrich, 96% purity), acridine (Aldrich, 97% purity), 1-methylanthracene (Aldrich, 99% purity), and 9-methylanthracene (Aldrich, 98% purity). All samples were used without further purification. Matheson prepurified argon (99.998% min) was used in these studies. The argon deposition line was liquid nitrogen trapped to further minimize contamination.

These PAHs have insufficient vapor pressure at room temperature to permit their preparation as a gaseous mixture with argon and thus have to be thermally vaporized before codeposition with larger amounts of argon. The PAHs were thermally vaporized by placing them in resistively heated Pyrex tubes mounted on the sample chamber. Sample temperatures were monitored using a chromel/alumel type K thermocouple mounted on the exterior of the tube. During PAH volatilization, argon was admitted through an adjacent inlet port in such a way that the two "streams" coalesced and froze together on the surface of the cold window.

Sample quality was found to be optimal for PAH deposition vapor pressures in the range from 10 to 30 mTorr. Optimum tube temperatures for the PAHs discussed here were: 9-cyanoanthracene, heated to 65 °C, 2-aminoanthracene, heated to 105 °C, acridine, maintained at room temperature, 1-methylanthracene, heated to 35 °C, and 9-methylanthracene, heated to 35 °C. The optimal argon flow rate was estimated to be between 0.5 and 1.0 mmol/h. On the basis of our argon flow rates and the PAH deposition rates estimated from measured band areas using the theoretical intrinsic band strengths presented later in this paper, we estimate the Ar/PAH ratios for our samples were all in excess of 2000/1. Thus, all of our PAH samples were well-isolated in argon.

After sample deposition, the cold head was rotated to face the beam of an infrared spectrometer and a spectrum was recorded and ratioed against a "blank" spectrum taken prior to sample deposition. The sample chamber was equipped with CsI vacuum windows and suspended in the sample compartment of an FTIR spectrometer (Nicolet Analytical Instruments, Model 740). Mid-infrared spectra (7000−500 cm^{-1}) were collected using an MCT-B detector/KBr beam splitter combination. All spectra reported here were measured at 0.5 cm^{-1} resolution. Spectra were typically generated through co-addition of 5 blocks of 200 scans, a number which optimized both the signal-to-noise ratio and time requirements of each experiment.

4. Results and Discussion

A. Overview. Since the theoretical data spans the full spectral range, we use simulated spectra based on the computed results to provide an overview and to demonstrate the overall good agreement between theory and experiment. In Figure 2, we compare simulated spectra for neutral anthracene and methyl-substituted anthracene. Adding a methyl side group in either the 1 or 9 position has little impact on the spectra apart from introducing the characteristic methyl C−H stretching bands in the 3000−2850 cm^{-1} range. The C−C stretch and C−H bending regions (400−1600 cm^{-1}) become a little more complex for the substituted system, because the lower symmetry mixes the bands that were allowed with those that were forbidden in

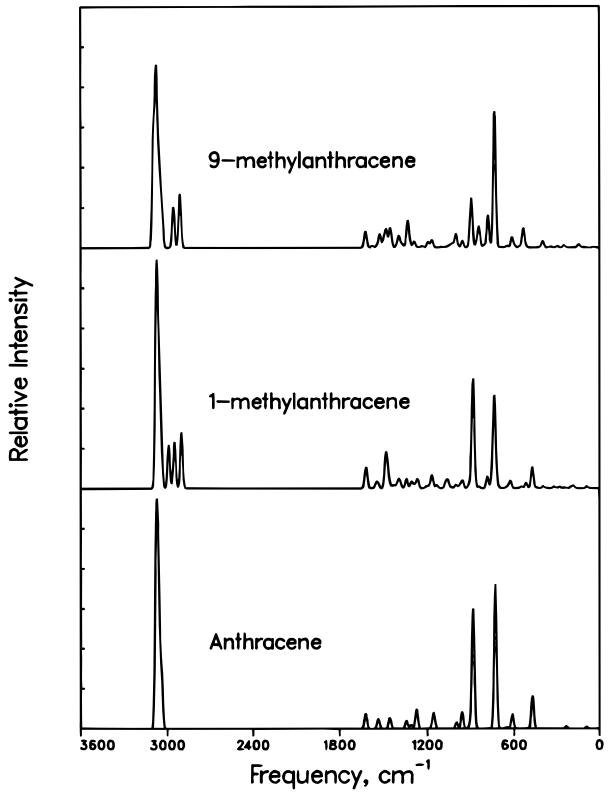

Figure 2. The theoretical IR spectra of anthracene, 1-methylanthracene, and 9-methylanthracene. The B3LYP frequencies are scaled by 0.958. Note that for all plots in this manuscript one tick on the *y* axis represents a constant unit of intensity and the full width at half-maximum (fwhm) is assumed to be 20 cm^{-1}.

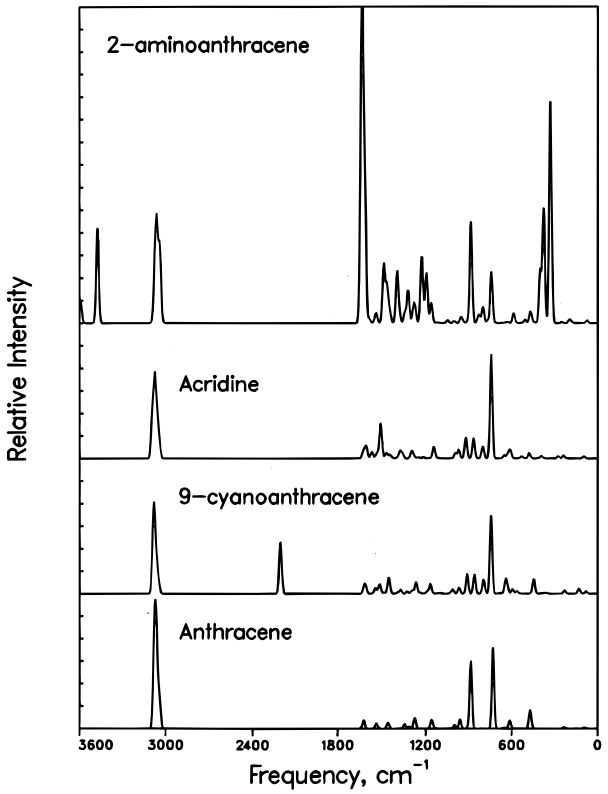

Figure 3. The theoretical IR spectra of anthracene, 9-cyanoanthracene, 2-aminoanthracene, and acridine. The B3LYP/4-31G are frequencies scaled by 0.958.

the higher symmetry anthracene. In Figure 3, we compare the spectrum of neutral anthracene with 2-amino- and 9-cyano-substituted anthracene and with acridine (nitrogen substitution in the ring at the 9 position). As observed with methyl substitution, the spectra of anthracene and acridine are very similar, except that the lower symmetry in acridine splits bands in the C−C stretching and C−H bending region of the spectrum. Replacing a ring H with CN also has little effect on the spectrum, other than introducing the C≡N stretch and splitting the C−C stretching and C−H bending regions. On-the-other-hand, replacing a hydrogen with NH_2 dramatically affects the spectrum. In addition to splitting the bands in the C−C stretching and C−H bending regions, NH_2 substitution increases the intensity of these bands greatly, in analogy with that observed upon ionization.[8] However, the addition of NH_2 does not reduce the C−H stretch intensity as dramatically as ionization.

In Figures 4 and 5 we show the analogous simulated spectra for the positive ions, as was shown for the neutrals in Figures 2 and 3, respectively. Relative to the neutrals there is a dramatic decrease in the intensities of the C−H and C≡N stretches and a dramatic increase in the intensity of the C−C stretches and C−H in-plane bends. Note that the intensity scale is significantly larger for the ions than the neutrals. Due to the larger intensity scale, the small differences between anthracene and the substituted systems, excluding 2-aminoanthracene, in the C−C stretching and C−H bending regions are less apparent for the ions than the neutrals. The spectrum for 2-aminoanthracene cation is still quite distinct. For the C−C stretching and C−H bending regions, there are more bands with sizable intensity and they cover a larger spectral range. Also in the higher frequency region, the N−H stretch is not decreased in intensity upon ionization as is the C−H and C≡N stretches.

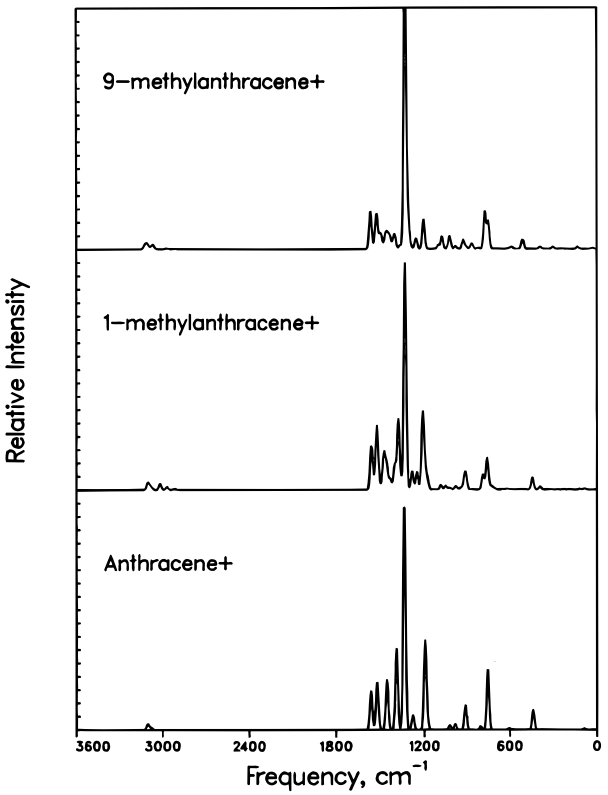

Figure 4. The theoretical IR spectra of the cations of anthracene, 1-methylanthracene, and 9-methylanthracene. The B3LYP frequencies are scaled by 0.958.

Before comparing the theoretical and experimental data and making band assignments for several substituted anthracenes,

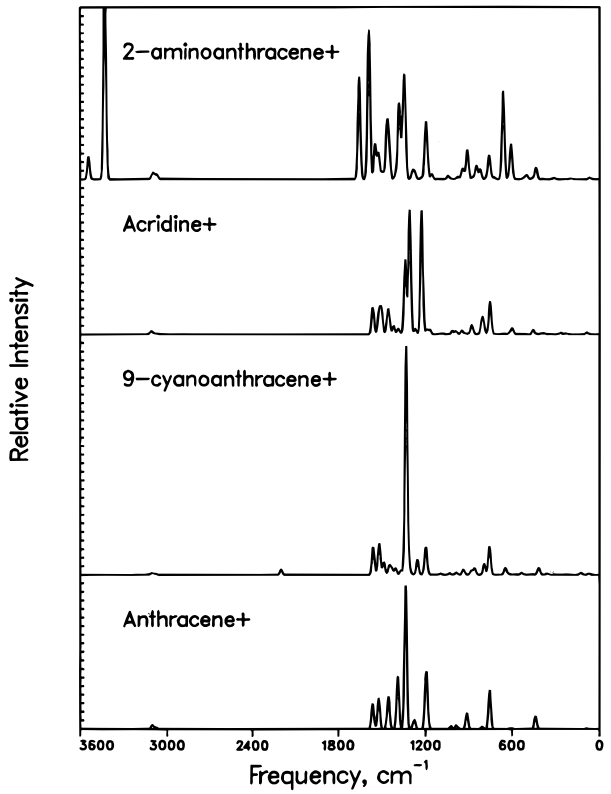

Figure 5. The theoretical IR spectra of the cations of anthracene, 9-cyanoanthracene, 2-aminoanthracene, and acridine. The B3LYP/4-31G frequencies are scaled by 0.958.

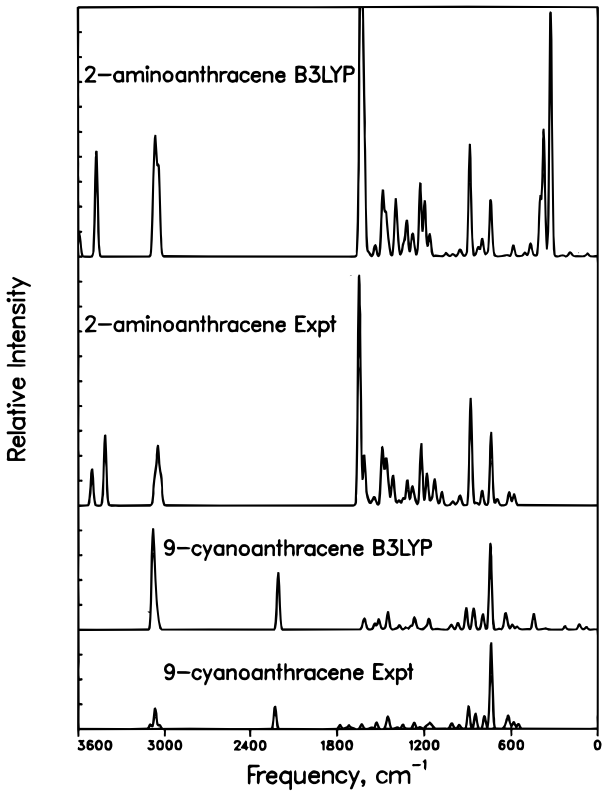

Figure 6. A plot of the theoretical and experimental data for neutral 9-cyanoanthracene and 2-aminoanthracene, using the data from the tables and assuming bandwidths of 20 cm^{-1} for both. Note that no experimental data is available below 500 cm^{-1}.

it is useful to compare the theoretical data for neutral anthracene and 9-cyanoanthracene. We choose these systems because of the high symmetry of the molecules and the perturbation of the CN group is sufficiently small that it is relatively unambiguous to make a one-to-one correspondence between the harmonic frequencies. In Table 1 we compare the frequencies and intensities of the harmonics of these two systems. The anthracene molecule has D_{2h} symmetry, whereas the 9-cyanoanthracene has C_{2v} symmetry. We do not include the b_{1g} and a_u modes of anthracene, which correspond to the a_2 modes of 9-cyanoanthracene, because they have zero intensity by symmetry. We can make the following approximate designation of the harmonics: 0−400 cm^{-1} (ring deformation and −C−N bend), 400−1000 cm^{-1} (C−H out-of-plane bend), 1000−1300 cm^{-1} (C−H in-plane bend), 1300−1620 cm^{-1} (C−C stretch), 2200 cm^{-1} (C≡N stretch), and 3030−3100 cm^{-1} (C−H stretch). The sums of the integrated intensities for anthracene and CN-substituted anthracene are very comparable. In other words, the small increase in intensity for the ring deformation, C−H in plane bend, and C−C stretch modes plus the addition of the relatively intense C≡N stretch mode in 9-cyanoanthracene nearly cancels the reduction in C−H stretch intensity compared with anthracene. The approximately 37% reduction in C−H stretch intensity is clearly not entirely due to having one fewer C−H bond. Instead the CN group withdraws some charge from the anthracene giving it a small positive charge. Recall that the C−H stretch intensities for the anthracene cation have much reduced C−H intensities and much enhanced C−H in-plane and C−C stretch intensities.

It is generally possible to make an unambiguous comparison of the modes of anthracene and 9-cyanoanthracene. There are, of course, some additional modes due to the CN group (e.g., the b_1 mode at 110.3 cm^{-1} and the b_2 mode at 128.9 cm^{-1} are due to CN out-of-plane and in-plane bends, respectively. Also the mode at 2203.7 cm^{-1} is clearly due to the C≡N stretch. Since one of the C−H bonds is replaced by a C−CN bond, there is one less symmetric C−H stretch mode in the substituted system. Overall the presence of the CN group in the nine position lowers the symmetry and spreads out the intensity into more bands. This is particularly noticeable for the "solo" out-of-plane bend modes, which in the unsubstituted case is concentrated in the b_{3u} mode at 885.3 cm^{-1}, while in the CN substituted anthracene, the one solo hydrogen band mixes with another band, causing the intensity to be distributed into two nearly equally intense bands at 860.6 and 912.4 cm^{-1}. The overall intensity of this band is reduced as there is now only one solo hydrogen and the band that it mixes with is forbidden in anthracene. While there are significant differences, the spectra are qualitatively similar in appearance and overall intensity—see Figure 3.

B. Comparison of Neutral Spectra. We should first note that there is good overall agreement between the DFT and experimental band positions and relative intensities, with the one exception that the theoretical C−H stretching intensities are about a factor of 2 too large. The agreement between theory is illustrated in Figure 6 where we plot the theoretical and the experimental data using the same full width at half-maximum for two representative systems. The good agreement in both the position and intensities gives us confidence that we can assign most of the experimental bands, although there are cases noted below where the assignment is ambiguous. We should also note that the experimental bands corresponding to C−H stretching modes are sufficiently overlapping and the theoretical bands too close in energy to make symmetry assignments of the bands. Thus, we compare only the total experimental and theoretical relative intensities for these bands.

TABLE 1: Comparison of the Theoretical Infrared Frequencies and Intensities for Neutral Anthracene and 9-Cyanoanthracene

anthracene			9-cyanoanthracene		
irreducible representation	frequency[a]	intensity[b]	irreducible representation	frequency[a]	intensity[b]
b_{3u}	91.0	1.03(0.01)	b_1	79.4	2.21(0.03)
			b_1	110.3	0.37(0.01)
			b_2	128.9	4.62(0.06)
b_{1u}	232.3	1.29(0.02)	a_1	227.8	3.03(0.04)
b_{2g}	267.1	*c*	b_1	270.6	0.28(<0.01)
b_{3u}	379.8	0.05(<0.01)	b_1	364.5	0.92(0.01)
a_g	390.2		a_1	386.4	0.17(<0.01)
b_{3g}	390.9		b_2	391.3	0.19(<0.01)
b_{3u}	471.3	17.29(0.23)	b_1	446.5	13.56(0.18)
			a_1	459.7	0.00(0.00)
b_{3g}	530.5		b_2	469.5	0.04(<0.01)
b_{2g}	584.4		b_1	562.1	2.29(0.03)
b_{2u}	612.7	7.53(0.10)	b_2	594.0	4.08(0.06)
			b_2	631.4	6.15(0.08)
			b_1	642.0	9.93(0.13)
a_g	637.9		a_1	648.1	1.47(0.02)
b_{1u}	651.6	0.62(0.01)	a_1	683.9	0.41(0.01)
b_{3u}	730.2	76.42(1.00)	b_1	743.8	73.87(1.00)
a_g	742.9				
b_{2g}	767.1		b_1	796.0	13.39(0.18)
b_{2u}	795.9	0.01(<0.01)	b_2	849.8	0.13(<0.01)
b_{1u}	908.0	1.67(0.02)	a_1	855.3	0.80(0.01)
b_{2g}	836.3				
b_{3u}	885.3	63.92(0.84)	b_1	860.6	17.45(0.24)
b_{2g}	909.9		b_1	912.4	18.54(0.25)
b_{3g}	918.3		b_2	931.9	0.00(0.00)
b_{3u}	962.0	8.64(0.11)	b_1	968.9	5.76(0.08)
b_{2g}	990.6		b_1	999.5	0.04(<0.01)
a_g	1005.4		a_1	1011.4	0.70(0.01)
b_{2u}	1000.7	3.20(0.04)	b_2	1013.7	2.88(0.04)
			a_1	1024.6	0.82(0.01)
b_{3g}	1100.4		b_2	1105.1	0.54(0.01)
b_{2u}	1157.7	3.37(0.04)	b_2	1167.9	4.73(0.06)
b_{1u}	1156.2	4.70(0.06)	a_1	1168.4	4.39(0.06)
a_g	1181.2		a_1	1188.1	0.20(<0.01)
b_{2u}	1169.3	0.98(0.01)	b_2	1190.7	1.94(0.03)
b_{3g}	1202.0		b_2	1239.7	0.96(0.01)
a_g	1265.9		a_1	1266.8	10.84(0.15)
b_{1u}	1274.6	10.19(0.13)	a_1	1293.5	3.24(0.04)
b_{3g}	1282.1				
b_{1u}	1311.2	1.96(0.03)	a_1	1328.3	1.80(0.02)
b_{2u}	1342.6	4.15(0.05)	b_2	1319.4	0.20(<0.01)
b_{2u}	1383.2	0.07(<0.01)	b_2	1372.9	3.70(0.05)
a_g	1385.2		a_1	1392.7	0.28(<0.01)
b_{3g}	1397.1		b_2	1397.9	0.58(0.01)
b_{2u}	1455.3	3.59(0.05)	b_2	1450.8	9.10(0.12)
b_{1u}	1456.1	2.05(0.03)	a_1	1453.8	6.32(0.09)
a_g	1481.9		a_1	1483.7	0.79(0.01)
b_{2u}	1533.7	4.95(0.06)	b_2	1513.4	8.92(0.12)
a_g	1541.0		a_1	1541.6	5.31(0.07)
b_{3g}	1578.0		b_2	1565.8	0.14(<0.01)
b_{3g}	1617.2		b_2	1608.8	6.75(0.09)
b_{1u}	1620.0	7.88(0.10)	a_1	1619.3	4.83(0.07)
			a_1	2203.7	48.97(0.66)
b_{1u}	3039.0	10.68(0.14)	a_1	3046.1	3.59(0.05)
a_g	3041.1				
b_{3g}	3043.4		b_2	3051.7	0.05(<0.01)
b_{1u}	3044.1	18.69(0.24)	a_1	3052.5	5.41(0.07)
b_{2u}	3047.5	0.01(<0.01)	b_2	3062.2	1.24(0.02)
a_g	3049.0		a_1	3062.4	17.80(0.24)
b_{3g}	3062.9		b_2	3075.2	8.98(0.12)
b_{1u}	3063.2	81.34(1.06)	a_1	3075.4	31.13(0.42)
b_{2u}	3077.8	95.47(1.25)	b_2	3086.0	62.04(0.84)
a_g	3078.4		a_1	3086.5	0.00(0.00)

[a] Theoretical frequencies are scaled by 0.958 (in cm^{-1}). [b] The absolute values (in km/mol) are given first with relative values in parentheses. [c] For anthracene the "g" modes are forbidden, but become allowed with substitution.

The original measured laboratory infrared spectra of all of the species discussed in this paper can be found in Figures 7 and 8. All the compounds were isolated in argon at T ≃ 10 K. Bands due to contaminant H_2O are labeled with dots (●).

In the comparisons of the theoretical and experimental spectra that follow, the reader will note that theory frequently predicts bands that are not observed in the laboratory data. However, in the vast majority of these cases the bands are predicted to be

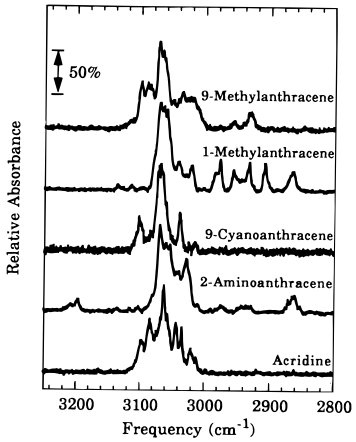

Figure 7. Experimentally measured infrared spectra through the aromatic C−H stretching region for the matrix-isolated, neutral forms of the five compounds discussed in this paper. Absorbance values are normalized to the most intense feature in the region. In all cases the Ar/PAH ratio is in excess of 2000/1.

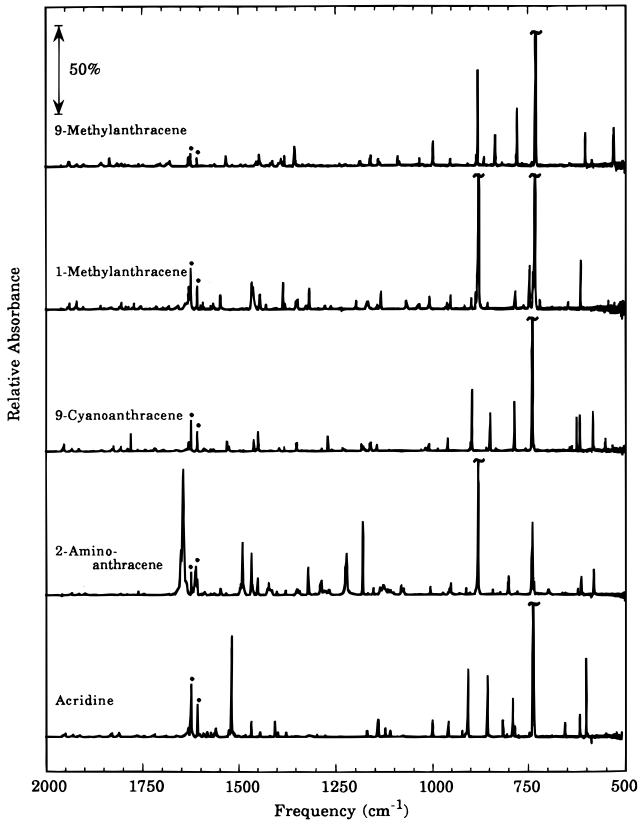

Figure 8. Experimentally measured infrared spectra in the 2000−500 cm^{-1} region for the matrix-isolated, neutral forms of the five compounds discussed in this paper. Absorbance values are normalized to the most intense feature in the aromatic C−H out-of-plane bending region (900−700 cm^{-1}). The strongest band(s) in each spectrum have been truncated at the 75% level to enhance the appearance of weaker features in the spectra. In all cases the Ar/PAH ratio is in excess of 2000/1. A "●" indicates the position of bands which arise from H_2O contaminant in the matrix.

very weak and they may not have been detected in the laboratory data due to insufficient signal-to-noise. We should note that we have not reported theoretical bands that are weaker than 0.1% of the strongest band, because it is highly unlikely that such bands will be observed. Also note that due to limitations in the experimental apparatus, no bands below 500 cm^{-1} are observed. Cases where stronger bands are predicted and not observed will be noted as we proceed. In addition, the laboratory data contain a substantial number of bands not predicted by theory, especially in the 1950−1500 cm^{-1} region. As for the case of unfunctionalized PAHs, we believe that these higher frequency bands are overtones and combinations of lower frequency fundamentals.[31] These bands are included in the tables and simulated spectra, but not discussed in detail. All experimental bands having intensities of 1% or greater than that of the strongest C−H out-of-plane bending mode are reported in the Tables.

The theoretical and matrix isolation bands of 9-cyanoanthracene are compared in Table 2. The experimental frequencies are in ascending order except for the bands observed at 847.5 and 857.1 cm^{-1}, which we have switched based on comparison with the theoretical relative intensities. Overall the agreement between theory and experiment is excellent both in band position and relative intensity. The largest differences are that experimentally the relative intensity of the C≡N stretch mode is a little more than a factor of 2 less intense than theory and the experimental C−H stretch intensity is much less than theory. For neutral anthracene, the sum of the DFT relative intensities for C−H stretch was about a factor of 3.4 larger than those in matrix isolation. Up to about a factor of 2 error was ascribed to theory and the remaining error to an underestimation of C−H stretch in the matrix. For CN−substituted anthracene the sum of the DFT intensities is a factor of 5.2 larger than experiment, even though we obtain an overall 37% reduction in absolute magnitude relative to anthracene. If this difference is meaningful, it may indicate that we are underestimating the electron withdrawing power of the CN group. If the DFT approach has underestimated the CN electron withdrawing, the true spectra will have weaker C−H stretches, but stronger C−C stretches and C−H bends than predicted by theory. As noted above, a complete assignment is not possible, for example, the band at 638.1 or the one at 643.2 cm^{-1} could be assigned as a_1 (with the computed result being at 648.1 cm^{-1}). It is also possible that these two experimental bands correspond to a_1 with a small site splitting, but one fundamental and an overtone or combination band cannot be ruled out. Similarly, a definitive assignment of the experimental bands at 1347.5 and 1348.7 cm^{-1} is not possible; we have scaled theoretical harmonics at 1328.3 and 1372.9 cm^{-1}. In this case it is possible that the experimental band is a superposition of the two DFT bands, one of which is too low in frequency and one of which is too high. It is also clear from the results presented in the table that several overtones and/or combination bands are observed in experiment. However, despite these few ambiguities, theory is capable of assigning most of the experimental bands.

The IR bands obtained from the DFT calculations and from the matrix-isolation spectra for 1-methylanthracene and 9-methylanthracene are compared in Tables 3 and 4. The methyl group, apart from reducing the symmetry and spreading the intensity into more bands, does not significantly change the intensity distribution in anthracene. For example, the "quartet" out-of-plane-bend band at 730.2 cm^{-1} (relative intensity = 1.00) in anthracene is split into three bands 712.1/733.9/748.1 with relative intensities of 0.026/0.864/0.192 in 1-methylanthracene. The solo out-of-plane-bend band in anthracene at 885.3 cm^{-1} (relative intensity = 0.84) is split into two bands at 883.0/891.4 cm^{-1} with relative intensities of 0.962/0.177 in 1-methylanthracene. Not surprisingly, introducing a methyl in the 1-position reduces the quartet out-of-plane-bend significantly, making

TABLE 2: Infrared Frequencies and Relative Intensities for Neutral 9-Cyanoanthracene

	theory		experiment	
irreducible representation	frequency[a]	relative intensity[b]	frequency	relative intensity
b_1	79.4	0.030		
b_1	110.3	0.005		
b_2	128.9	0.063		
a_1	227.8	0.041		
b_1	270.6	0.004		
b_1	364.5	0.013		
a_1	386.4	0.002		
b_2	391.3	0.003		
b_1	446.5	0.184		
b_2	469.5	0.001		
b_1	562.1	0.031	552.5	0.056
b_2	594.0	0.055	584.2	0.075
b_2	631.4	0.083	618.1	0.100
b_1	642.0	0.134	625.8	0.064
a_1	648.1	0.020	638.1	0.016
			643.2	0.017
a_1	683.9	0.006		
b_1	743.8	1.000	738.5	1.000
b_1	796.0	0.181	784.8	0.150
b_2	849.8	0.002		
a_1	855.3	0.011	857.1	0.010
b_1	860.6	0.236	847.5	0.170
b_1	912.4	0.251	894.9	0.260
b_1	968.9	0.078	959.2	0.045
b_1	999.5	0.001		
a_1	1011.4	0.009		
b_2	1013.7	0.039	1008.8	0.041
a_1	1024.6	0.011	1014.3/1018.3	0.026
b_2	1105.1	0.007		
			1144.3	0.031
b_2	1167.9	0.064	1160.4/1163.4	0.064
a_1	1168.4	0.059	1179.6	0.013
a_1	1188.1	0.003		
b_2	1190.7	0.026	1182.7/1184.3	0.027
b_2	1239.7	0.013	1226.8/1231.8	0.021
a_1	1266.8	0.147	1268.2/1269.0	0.072
a_1	1293.5	0.044		
b_2	1319.4	0.003		
a_1	1328.3	0.024	1347.5/1348.7	0.048
b_2	1372.9	0.050		
a_1	1392.7	0.004	1392.8	0.017
b_2	1397.9	0.008		
b_2	1450.8	0.123	1448.0/1448.8	0.120
a_1	1453.8	0.086	1459.4	0.052
a_1	1483.7	0.011		
b_2	1513.4	0.121	1524.2	0.018
a_1	1541.6	0.072	1529.6/1531.5	0.059
b_2	1565.8	0.002	1566.5	0.016
b_2	1608.8	0.091		
a_1	1619.3	0.065	1630.2	0.054
			1694.6[c]	0.011
			1718.2[c]	0.041
			1740.9/1743.6[c]	0.012
			1779.3[c]	0.045
a_1	2203.7	0.663	2224.3/2226.2	0.260
a_1	3046.1	0.049	3037.5	0.045
b_2	3051.7	0.001		
a_1	3052.5	0.073		
b_2	3062.2	0.017		
a_1	3062.4	0.241	3067.4	0.240
b_2	3075.2	0.122		
a_1	3075.4	0.421		
b_2	3086.0	0.840	3101.6	0.053

[a] Theoretical frequencies (in cm^{-1}) are scaled by 0.958. [b] The absolute intensities (in km/mol) can be obtained by multiplying by the factor of 73.87. [c] These are likely overtone or combination bands.

it less than the solo band. Conversely, introducing the methyl at the solo position (9 position) greatly reduces the solo band intensity.

The theoretical and experimental spectra for 1-methyl and 9-methylanthracene are in excellent agreement. In most cases there is a clear correspondence of theory and experiment, but the assignment of a few bands is uncertain; for example, in 1-methylanthracene, the experimental band at 1069.3 cm^{-1} may be assigned to either the theoretical band at 1058.6 or 1073.4 cm^{-1}. The same uncertainty applies to assignment of the experimental band at 1442.7 cm^{-1} and the bands at 1444.7 and 1561.6 cm^{-1} in 9-methylanthracene. Also, as noted above, the experimental spectrum contains a significant number of overtone and combination bands observed between 1650 and 1950 cm^{-1}. These bands will likely become even more intense as the vibrational temperature increases. The relative intensities in the theoretical and experimental spectra generally agree well (better than a factor of 2) especially in the CH out-of-plane bend regions. The spectra in the C−C stretch and C−H in-plane bend regions are weaker and more complex resulting in somewhat greater differences. Nevertheless, the agreement overall is very satisfactory.

The theoretical and matrix isolation spectra of 2-aminoanthracene are compared in Table 5. Due to the cutoff in the spectrometer band-pass, the lowest frequency band observed experimentally is at 581.7 cm^{-1}, which we correlate to our scaled harmonic at 586.5 cm^{-1}. As can be seen from Table 5, the strongest harmonic is at 329.5 cm^{-1}. The band at 1644.5 cm^{-1} is the strongest band observed experimentally. This is the second strongest band in theory and has a relative intensity of 0.99. As a result of the two band having nearly equal intensity, no significant complications arise from theory and experiment being normalized using different bands. In addition to the strong band at 329.5 cm^{-1}, there are several other strong harmonics between about 320 and 400 cm^{-1}. This is markedly different from the spectra of anthracene, 1-methylanthracene, 9-methylanthracene, and 9-cyanoanthracene, where only weak bands are observed below 400 cm^{-1}. We attribute these bands to out-of-plane bending motions of the NH_2 group. Experimentally, there are two moderately strong bands at 697.9 and 1076.6/1082.1 cm^{-1} for which no theoretical harmonic correlates. We believe that these may be combination bands, for example, the band at 697.9 cm^{-1} may be a combination of the strong theoretical a″ bands calculated at 329.5 and 376.7 cm^{-1} and similarly the 1076.6/1082.1 cm^{-1} bands may be due to a combination of the 329.5 and 741.5 a″ harmonics. We have correlated the experimental bands at 1128.2, 1136.8, and 1153.7 cm^{-1} with the a′ harmonics at 1159.5, 1163.1, and 1174.9 cm^{-1}, although the discrepancies in the frequencies are larger than we would expect. In this regard we should note that the 1076.6/1082.1 cm^{-1} band could correlate with the DFT scaled harmonic at 1049.6 cm^{-1}. While the difference between theory and experiment is larger than expected, this is the region of the spectrum where theory and experiment seem to differ most. The experimental band at 1494.2 may be a site splitting of the relatively intense band at 1489.3 cm^{-1}, although this is a large matrix shift.

The sum of the C−H stretch intensities for 2-aminoanthracene are comparable to that of unsubstituted anthracene, even though there is one less C−H bond. The sum of the theoretical relative intensities is about twice that of experiment, which can be accounted for on the basis of the expected overestimation at this level of theory. The two N−H stretch modes are also quite intense, and theory and experiment are in relatively good agreement on their relative intensity. The errors in the theoretical frequencies are larger than for the other modes. Part of this difference arises from the larger anharmonicity in N−H compared with C−H bonds and part from the greater basis set requirements for accurately describing the NH stretch compared with the CH stretch. Hence, the DFT/4-31G frequencies scaled

TABLE 3: Infrared Frequencies and Relative Intensities for Neutral 1-Methylanthracene

	theory		experiment			theory		experiment	
mode	frequency[a]	relative intensity[b]	frequency	relative intensity	mode	frequency[a]	relative intensity[b]	frequency	relative intensity
1	89.0	0.018			42	1287.1	0.031	1315.5	0.073
2	178.8	0.022			43	1307.3	0.064	1324.4/1321.0	0.023
3	196.2	0.012			44	1342.7	0.090	1344.9/1348.0	0.068
4	197.8	0.006			45	1377.0	0.007		
5	242.8	0.007			46	1385.5	0.017	1377.2	0.017
6	282.5	0.013			47	1391.4	0.072	1382.5	0.077
7	316.7	0.016			48	1406.7	0.041		
8	386.6	0.001			49	1431.2	0.033	1426.8	0.025
9	394.7	0.018			50	1457.3	0.046		
10	443.3	0.007			51	1473.4	0.156	1442.7	0.083
11	471.4	0.206			52	1475.7	0.078		
12	516.0	0.051			53	1485.3	0.206	1463.8 complx	0.317
13	547.8	0.016			54	1536.6	0.050	1547.5	0.055
14	585.6	0.001			55	1549.2	0.034	1566.2	0.037
15	626.0	0.074	615.9	0.080	56	1579.2	0.002		
16	647.6	0.015	647.1	0.013	57	1613.5	0.062	1599.7	0.014
17	712.1	0.026	719.8	0.029	58	1618.4	0.150	1629.8	0.060
18	733.9	0.864	731.2/737.5	0.980				1657.4[d]	0.039
19	748.1	0.192	745.4	0.139				1681.6[d]	0.019
20	762.3	0.001						1714.2[d]	0.019
21	777.4	0.007	761.0	0.011				1753.1 complx[d]	0.026
22	784.2	0.107	781.8	0.077				1770.4[d]	0.015
23	844.5	0.001						1803.4/1808.5[d]	0.038
24	845.2	0.016	853.9	0.021				1829.4[d]	0.012
25	883.0	0.962	877.5 complx[c]	1.000				1856.7/1859.1[d]	0.014
26	891.4	0.177	896.5	0.025				1919.6/1924.6[d]	0.052
27	910.6	0.027						1938.1/1943.3[d]	0.034
28	915.0	0.005						2864	0.104
29	958.0	0.073	951.9/955.3	0.043	59	2900.1	0.551	2907	0.094
30	976.1	0.029	961.3/965.9	0.019	60	2948.6	0.454	2932	0.192[e]
31	1003.1	0.031	1007.3/1011.8	0.062	61	2989.6	0.427	2976/2983.8	0.142
32	1034.5	0.010	1035.8 complx	0.037	62	3039.1	0.136		
33	1058.6	0.070			63	3043.0	0.115		
34	1073.4	0.057	1069.3	0.059	64	3044.4	0.028		
35	1134.8	0.030	1134.2/1138.1	0.066	65	3047.4	0.009		
36	1165.4	0.035	1143.3/1144.3	0.013	66	3052.2	0.569		
37	1170.0	0.091	1166.8 complx	0.085	67	3062.8	0.586		
38	1182.5	0.017			68	3067.2	0.345		
39	1202.9	0.021	1197.0	0.032	69	3073.4	1.000	3069	1.23[e]
40	1263.4	0.013	1261.3	0.015	70	3078.2	0.797		
41	1268.4	0.078	1275.4	0.030					

[a] Theoretical frequencies (in cm^{-1}) are scaled by 0.958. [b] The absolute intensities (in km/mol) can be obtained by multiplying by the factor of 53.918. [c] Signifies a complex (complx) absorption feature that is composed of multiple overlapping, incompletely resolved bands whose strengths cannot be measured individually. [d] These are likely overtone or combination bands. [e] Integrated intensity for 2956 (w/2932), 3019 (w/3069), 3040 (w/3069) 3058 (w/3069), and 3063 (w/3069).

by 0.958 are not as accurate as the other modes. However, their frequencies are sufficiently distinct that their identification is unambiguous.

One unique aspect of the 2-aminoanthracene neutral spectrum is the great strength of the modes between 1300 and 1650 cm^{-1}. This is due to two factors. First, the in-plane bending motions of the NH_2 group, which appear in the theoretical spectrum between 1610 and 1640 cm^{-1}, are very intense. The experimental spectrum agrees reasonably well with the theoretical one in this spectral region, although the relative intensity is about a factor of 2 less in the matrix isolation spectrum. Second, the NH_2 group is very electron withdrawing and induces a partial positive charge on the ring carbons that enhances the C−C stretch modes, reminiscent of the cation spectra.[8] The sum of the absolute theoretical intensities for 2-aminoanthracene is 1748 km/mol compared with 432 km/mol for anthracene itself. This enhancement by a factor of 4 in total intensity is not only due to the NH_2 motions, but also to the larger charge localization on the ring atoms. The Mulliken populations indicate a partial positive charge of 0.31 electrons on the ring carbon to which the NH_2 group is attached. In contrast, the carbon to which the CN group is attached in 9-cyanoanthracene has a partial positive charge of less than 0.01 electrons and hence the CN spectrum looks more like anthracene than 2-aminoanthracene.

The theoretical and matrix-isolation spectra of acridine (nitrogen substitution in anthracene at the nine position—see Figure 1) are compared in Table 6. Comparing first the theoretical acridine spectrum with the anthracene spectrum in Table 1 we can make the following observations. The strong out-of-plane C−H bend mode derived from the quartet hydrogens, which in anthracene is at 730.2 cm^{-1}, is shifted to 742.8 cm^{-1} and is increased in intensity by about 30%. The out-of-plane C−H bend due to the solo hydrogens, which in anthracene appears as a strong band at 885.3 cm^{-1}, appears as two nearly equally intense peaks in acridine at 866.6 and 921.1 cm^{-1}. Overall, the sum of the out-of-plane bending modes are about equal for anthracene and acridine. The C−H in-plane bend modes between about 1000 and 1300 cm^{-1} are comparable and relatively weak in both systems. However, the region between 1300 and 1620 cm^{-1} is significantly enhanced in acridine, with a new, relatively intense band appearing at 1507.1 cm^{-1}. The larger intensity results from a larger change in dipole moment

TABLE 4: Infrared Frequencies (cm^{-1}) and Relative Intensities for Neutral 9-Methylanthracene

	theory		experiment			theory		experiment	
mode	frequency[a]	relative intensity[b]	frequency	relative intensity	mode	frequency[a]	relative intensity[b]	frequency	relative intensity
1	36.9	0.004			44	1261.8	0.003	1239.5	0.010
2	101.8	0.002			45	1290.0	0.044		
3	111.0	0.001			46	1320.0	0.038		
4	143.5	0.024			47	1333.7	0.191	1352.1/1354.0	0.154
5	245.0	0.017			48	1368.8	0.023	1378.4/1380.7	0.046
6	294.4	0.012			49	1391.3	0.075	1387.4 complx[c]	0.079
7	339.9	0.006			50	1397.2	0.016	1409.5/1414.5	0.064
8	390.0	0.002			51	1408.5	0.014	1424.7	0.012
9	396.6	0.048			52	1450.4	0.098	1444.7	0.082
10	418.6	0.003			53	1452.8	0.051		
11	474.0	0.001			54	1474.1	0.035	1451.9	0.029
12	518.3	0.013			55	1479.9	0.100	1492.9	0.011
13	533.4	0.142	530.8	0.214	56	1495.0	0.061		
14	556.7	0.010			57	1522.9	0.100	1532.5	0.065
15	593.6	0.013	587.0	0.020	58	1543.1	0.012	1561.6	0.026
16	612.4	0.076	603.4	0.079	59	1573.3	0.014		
17	647.3	0.012			60	1610.5	0.001		
18	685.5	0.003			61	1619.2	0.121	1628.3/1630.5	0.063
19	732.4	1.000	728.9/730.1	1.000				1678.3[d]	0.048
20	740.6	0.030	738.8/739.8	0.011				1702.6[d]	0.020
21	756.1	0.003						1758.3/1757.3[d]	0.011
22	778.0	0.240	777.2/779.8	0.180				1785.1[d]	0.013
23	806.3	0.019	816.0	0.011				1792.5[d]	0.014
24	840.9	0.150	833.3	0.165				1802.4[d]	0.028
25	851.9	0.009						1812.2[d]	0.030
26	857.6	0.035	862.6	0.029				1833.0[d]	0.054
27	894.5	0.365	879.9/883.7	0.319				1854.5/1857.9[d]	0.050
28	906.0	0.011	906.4	0.009				1901.0[d]	0.015
29	952.5	0.006						1917.6[d]	0.023
30	957.5	0.045	952.5/954.8	0.025				1937.5/1940.0[d]	0.062
31	987.1	0.002			62	2908.8	0.401	2932	0.100[e]
32	989.1	0.002			63	2954.3	0.303		
33	1001.3	0.099	996.8/998.0	0.193	64	3034.8	0.223		
34	1015.7	0.003			65	3040.6	0.041		
35	1025.1	0.024			66	3044.4	0.001		
36	1041.5	0.017			67	3045.8	0.126		
37	1062.5	0.009	1086.2	0.013	68	3055.2	0.190		
38	1103.2	0.005	1090.6/1092.3	0.036	69	3055.6	0.281		
39	1167.2	0.023	1140.5/1136.9	0.050	70	3073.5	0.669	3035	1.13[e]
40	1169.4	0.033	1160.2/1162.9	0.056	71	3074.4	0.583		
41	1189.9	0.001			72	3091.0	0.405		
42	1194.5	0.039	1186.5/1188.7	0.035	73	3095.6	0.476		
43	1234.9	0.010	1226.0	0.011					

[a] Theoretical frequencies (in cm^{-1}) are scaled by 0.958. [b] The absolute intensities (in km/mol) can be obtained by multiplying by the factor of 70.691. [c] Signifies a complex (complx) absorption feature that is composed of multiple overlapping, incompletely resolved bands whose strengths cannot be measured individually. [d] These are likely overtone or combination bands. [e] Integrated intensity for 2956(w/2932), 3018(w/3035), 3065(w/3035), 3071(w/3035), 3089(w/3035), and 3099(w/3035).

as the ring is stretched. The Mulliken population on the ring nitrogen is −0.54 electrons for acridine. Finally, the sum of the C−H stretch intensities in acridine are reduced by about 20% compared with anthracene.

The theoretical and experimental spectra agree very well for acridine. In the out-of-plane bend region, the experimental frequencies are from 5 to 15 cm^{-1} less than the scaled DFT values, but the relative intensities agree very well. The weak band observed in the matrix at 745.6 cm^{-1} is probably due to site splitting in the matrix. The experimental spectrum is consistent with theory in finding a relatively strong band (at 1518.7 compared with 1507.1 cm^{-1}) due to stretching motions of the backbone, which must be ascribed to the presence of nitrogen in the ring due to its absence in unsubstituted anthracene. The experimental C−H stretch intensities are about a factor of 2 less than theory in acridine, which as has been mentioned before can be attributed to an overestimation of these intensities at the 4-31G/DFT level of theory. We should note that, as in other cases, some alternative assignments are possible. For example, the mapping of the theoretical bands at 801.0 and 802.1 cm^{-1} onto the three experimental bands between 783.4 and 815.0 cm^{-1} and similarly the mapping of the computed bands at 1605.0 and 1623.6 cm^{-1} onto the three experimental bands between 1601.4 and 1631.3 cm^{-1} is not unambiguous. Finally, we note that theory predicts bands at 1296.3 and 1360.0 cm^{-1} that are not observed in experiment, despite having an intensity larger than many of the observed bands. Despite any uncertainty in some of the assignments, overall the theoretical and matrix isolation spectra are in good accord.

C. Comparison of Cation Spectra. Whereas the theoretical and experimental neutral spectra agree very well, we find much less satisfactory agreement for the cation spectra. This is best illustrated by a plot of the data (see Figures 9 and 10). While the agreement is worse than that found for the neutrals, it is sufficiently good to convince oneself that theory and experiment are studying the same molecule. There may be several reasons for this poorer agrement. The DFT calculations may be less accurate for the cation species than the neutrals for the relative

TABLE 5: Infrared Frequencies (cm^{-1}) and Relative Intensities for Neutral 2-Aminoanthracene

	theory		experiment	
irreducible representation	frequency[a]	relative intensity[b]	frequency	relative intensity
a″	71.6	0.012		
a″	183.4	0.008		
a′	195.8	0.014		
a″	249.3	0.005		
a″	322.2	0.104		
a″	329.5	1.000		
a′	368.2	0.001		
a″	376.7	0.553		
a″	401.2	0.256		
a′	438.8	0.004		
a″	462.7	0.015		
a″	470.7	0.046		
a′	508.1	0.016		
a″	539.8	0.001		
a′	586.5	0.048	581.7	0.048
			613.9	0.053
a″	623.2	0.002	622.2	0.008
a′	632.2	0.005		
a′	658.5	0.001		
			697.9	0.028
a″	731.5	0.007		
a″	741.5	0.244	738.1	0.320
a″	760.5	0.001		
a′	767.6	0.010		
a″	799.9	0.076	799.6/801.5	0.064
a″	825.7	0.029		
a′	833.3	0.014		
a″	846.1	0.003	841.1	0.011
a″	884.8	0.490	879.4	0.470
a″	900.1	0.003		
a′	911.3	0.005		
a′	944.0	0.007		
a″	952.6	0.013		
a″	957.0	0.014	951.7/954.5	0.042
			972.5	0.009
a′	1003.5	0.009	1005.5	0.017
a′	1049.6	0.013		
			1076.6/1082.1	0.058
a′	1114.7	0.002	1110.3	0.010
a′	1159.5	0.012	1128.2	0.100
a′	1163.1	0.082	1136.8	0.021
a′	1174.9	0.011	1153.7	0.019
a′	1198.1	0.242	1181.2	0.140
a′	1228.7	0.321	1221.8	0.270
a′	1274.1	0.052	1266.2	0.022
a′	1281.1	0.004	1277.0	0.018
a′	1285.5	0.067	1284.9	0.069
a′	1322.1	0.156	1318.2	0.110
a′	1344.5	0.053	1346.1	0.031
a′	1381.2	0.017	1375.8	0.022
a′	1385.1	0.028	1399.4	0.010
a′	1398.7	0.242	1412.0/1424.0	0.130
a′	1447.8	0.057	1449.4	0.075
a′	1465.8	0.179	1465.2	0.190
a′	1487.2	0.283	1489.3	0.240
			1494.2	0.017
a′	1531.7	0.002	1533.0	0.008
a′	1539.7	0.049	1547.3	0.033
			1562.3/1565.4	0.011
a′	1584.2	0.019	1589.1	0.022
a′	1613.3	0.476	1598.7/1602.1	0.009
a′	1628.4	0.914	1611.7/1613.6	0.220
			1638.1	0.022
a′	1639.8	0.990	1644.5/1650.7	1.000
a′	3035.1	0.064		
a′	3036.8	0.003		
a′	3038.9	0.049		
a′	3040.0	0.014		
a′	3041.1	0.247	3027.3/3068.4	0.500
a′	3044.9	0.004		
a′	3059.9	0.211		
a′	3060.8	0.234		
a′	3075.5	0.278		
a′	3474.8	0.461	3410.0/3420.6	0.310
a′	3591.8	0.102	3498.6/3512.8	0.160

[a] Theoretical frequencies (in cm^{-1}) are scaled by 0.958. [b] The absolute intensities (in km/mol) can be obtained by multiplying by the factor of 195.10.

TABLE 6: Infrared Frequencies and Relative Intensities for Neutral Acridine

	theory		experiment	
irreducible representation	frequency[a]	relative intensity[b]	frequency	relative intensity
b_1	93.2	0.020		
a_1	235.8	0.028		
b_1	273.8	0.020		
b_1	390.3	0.023		
b_2	414.0	0.004		
b_1	477.5	0.050		
b_2	530.2	0.020		
b_2	610.5	0.082	601.5	0.110
a_1	626.8	0.035	618.1	0.031
a_1	652.6	0.029	655.5	0.030
a_1	730.7	0.003		
b_1	742.8	1.000	736.0	1.000
			745.6	0.012
b_1	801.0	0.079	783.4	0.020
b_2	802.1	0.036	788.5	0.096
			813.3/815.0	0.040
b_1	866.6	0.192	854.3	0.170
a_1	899.8	0.001		
b_1	921.1	0.190	906.7	0.180
b_2	922.5	0.010	921.5	0.011
b_1	970.7	0.083	958.0	0.054
b_2	995.5	0.049	998.7/1000.2	0.050
b_1	1000.4	0.001		
b_2	1108.7	0.006	1110.1/1111.5	0.020
a_1	1144.0	0.098	1123.4	0.030
b_2	1150.2	0.017	1141.4/1142.7	0.081
b_2	1178.3	0.004	1169.8	0.025
b_2	1218.4	0.012		
a_1	1253.0	0.010		
a_1	1281.0	0.018		
b_2	1296.3	0.071		
b_2	1360.0	0.046		
a_1	1377.1	0.068	1375.4	0.020
b_2	1396.8	0.007	1395.8/1397.1	0.015
			1404.7	0.057
b_2	1442.7	0.032	1442.3/1443.4	0.024
a_1	1466.1	0.047	1466.6	0.050
a_1	1477.5	0.012	1511.2	0.008
b_2	1507.1	0.337	1518.7	0.350
a_1	1532.0	0.053	1525.7/1527.2	0.022
b_2	1567.4	0.062	1559.9/1564.9	0.083
			1581.2/1582.8	0.023
b_2	1605.0	0.117	1601.4	0.015
a_1	1623.6	0.077	1625.4	0.150
			1631.3	0.037
a_1	3042.7	0.021		
b_2	3045.6	0.005		
a_1	3046.8	0.140		
b_2	3060.2	0.006		
a_1	3060.3	0.323		
b_2	3075.8	0.568	3042.7	0.760[c]
a_1	3076.1	0.151		
b_2	3092.9	0.314		
a_1	3093.4	0.096		

[a] Theoretical frequencies (in cm^{-1}) are scaled by 0.958. [b] The absolute intensities (in km/mol) can be obtained by multiplying by the factor of 98.21. [c] Integrated intensity for 3097.4, 3083.0, 3061.0, 3042.7, 3033.3, and 3020.0

intensities because of the much greater importance of electron correlation for the ions, as demonstrated by the significant overestimate of the HF intensities for the cation in comparison with the good agreement at the same level of theory for the neutrals.[30] Second, in the matrix only a small amount of cation is formed so that the neutral peaks can mask many of the cation species, which results in missing cation bands or cation bands with uncertain strengths. Finally, irradiation by UV light can cause photolysis resulting in the presence of other species that

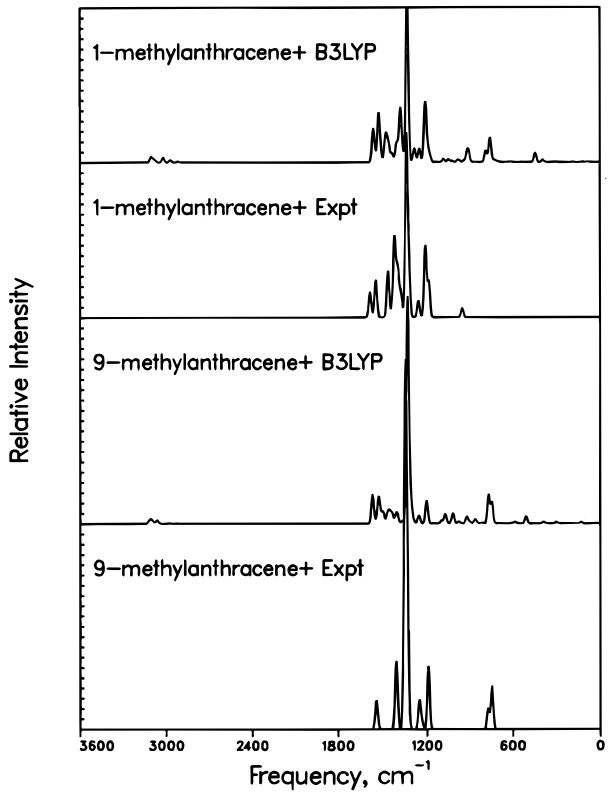

Figure 9. A comparison plot of the theoretical and experimental data for 1-methyl and 9-methylanthracene cations, using the data from the tables. Note that no experimental data is available below 500 cm^{-1}.

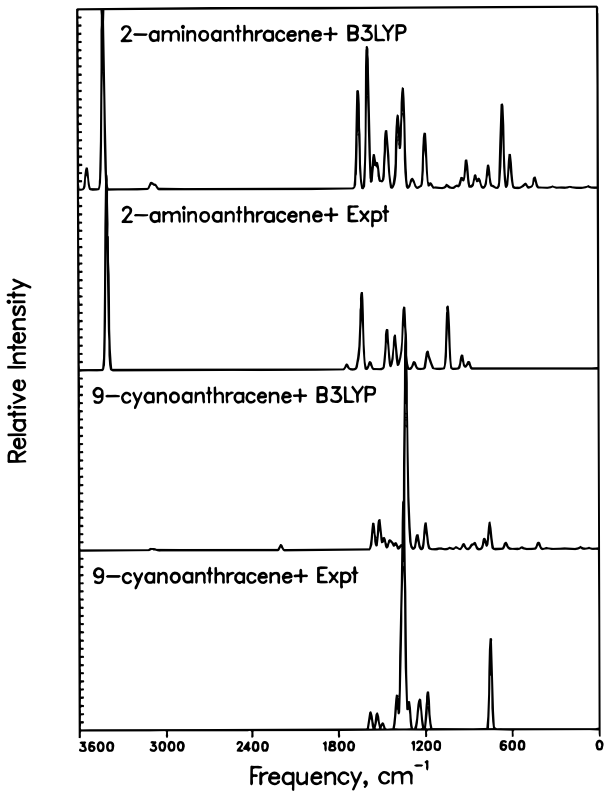

Figure 10. A comparison plot of the theoretical and experimental data for 9-cyanoanthracene and 2-aminoanthracene cations, using the data from the tables. Note that no experimental data is available below 500 cm^{-1}.

can contribute to the spectrum. The fact that many fewer lines are observed in experiment for the ions precludes a one-to-one correspondence between the theoretical and experimental bands. Often the computed bands can be assigned to the relatively few experimental bands in several different ways. Thus, the band assignments for the ions must be considered tentative, except for a few of the very strongest bands or for those widely separated from the others.

TABLE 7: Infrared Frequencies and Relative Intensities for the 9-Cyanoanthracene Cation

	theory		experiment	
irreducible representation	frequency[a]	relative intensity[b]	frequency	relative intensity
b_1	73.2	0.005		
b_2	128.6	0.008		
a_1	226.1	0.002		
b_1	359.1	0.004		
b_1	417.9	0.030		
a_1	455.9	0.001		
b_1	532.8	0.008		
b_2	587.3	0.001		
b_2	624.1	0.003		
b_1	645.6	0.029		
b_1	755.3	0.123	751.0	0.417
b_1	791.6	0.047		
a_1	851.3	0.001		
b_2	859.0	0.027		
b_1	881.0	0.018		
b_2	931.9	0.006		
b_1	939.0	0.019		
b_1	988.0	0.009		
a_1	1030.4	0.001		
b_2	1033.6	0.005		
b_2	1098.0	0.005		
b_2	1184.8	0.006		
a_1	1196.7	0.001		
b_2	1199.9	0.119	1187.0	0.170
			1239.3	0.087
			1248.4	0.049
b_2	1258.2	0.066	1255.9	0.048
a_1	1295.5	0.003		
a_1	1316.1	0.058	1320.7	0.126
b_2	1335.7	1.000	1353.3	1.000
b_2	1347.2	0.004		
a_1	1372.2	0.019	1370.2/1372.9	0.476
b_2	1408.9	0.029	1405.0	0.157
b_2	1435.1	0.027		
a_1	1452.4	0.038		
b_2	1489.0	0.052		
a_1	1495.4	0.004		
b_2	1520.0	0.113	1502.1	0.029
b_2	1526.9	0.031		
a_1	1542.8	0.002	1538.9	0.074
a_1	1562.5	0.121	1583.3	0.080
a_1	2197.0	0.023		
b_2	3078.4	0.001		
a_1	3084.8	0.002		
b_2	3106.8	0.007		
a_1	3106.9	0.001		

[a] Theoretical frequencies (in cm^{-1}) are scaled by 0.958. [b] The absolute intensities (in km/mol) can be obtained by multiplying by the factor of 562.90.

The DFT frequencies and relative intensities are compared with the matrix isolation results for 9-cyanoanthracene cation in Table 7. The strong out-of-plane b_1 C−H bend mode occurs at 755.3 (751.3) cm^{-1} theoretical (experimental) in 9-cyanoanthracene cation. This is an increase of 11.5 (12.5) cm^{-1} compared with the neutral. The experimental relative intensity is, however, a factor of over three larger than theory. This could be due to an overestimation of the intensity of the strong C−C stretch intensities at the DFT level. The out-of-plane bend due to the solo hydrogen is spread into several bands and not readily recognizable. Experimentally, this band cannot be distinguished

from the background spectrum of the neutral. Theory and experiment concur that the strongest band occurs for C−C stretch modes at 1335.7 and 1353 cm^{-1}, respectively. There is a relatively strong band observed at 1370.2/1372.9 cm^{-1} in the matrix that we correlate with an a_1 harmonic in Table 7. However, this band is rather weak in the theoretical spectrum. Experimentally, the relative intensity of this band does not significantly change as a function of time after UV irradiation. Thus, we cannot distinguish between the possibility that the intensity of this band is significantly underestimated at the DFT level or that this band originates from a species other than 9-cyanoanthracene cation.

The IR bands obtained from the DFT calculations and from the matrix isolation spectra for the cations of 1-methylanthracene and 9-methylanthracene are given in Tables 8 and 9. Although there is qualitative agreement between theory and experiment, clearly the quantitative agreement that was achieved for the neutrals is not achieved for the ions. For 1-methylanthracene the strongest band observed was the C−C stretch frequency at 1339.1 cm^{-1}, which agrees well with the calculated harmonic at 1333.4 cm^{-1}. It is unclear whether the relatively strong band observed at 1323.5 cm^{-1} is part of this complex. The experimental bands at 1210.6/1214.4 cm^{-1} are consistent with the strong harmonic at 1211.5 cm^{-1}, but the experimental bands at 1186.9 and 1418.9 cm^{-1} have no strong theoretical band that can be associated with them. For 9-methylanthracene there are also problems in making one-to-one correspondences between theory and experiment. For example, there is only one strong theoretical band at 1332.1 cm^{-1}, but four bands observed experimentally between 1332.7 and 1353.0 cm^{-1}. Again the experimental spectrum in the region above 1400 cm^{-1} is stronger than the theoretical one. Thus, only qualitative agreement between theory and experiment can be claimed for these methyl-substituted anthracene cations.

The DFT frequencies and relative intensities for 2-aminoanthracene are compared with the matrix-isolation values in Table 10. We first note that the intensity for the strongest band of the cation is 505.0 km/mol compared with 195.1 km/mol for the neutral. In the neutral, the out-of-plane bend of the hydrogens on the NH_2 moiety were very strong and occurred between about 320−400 cm^{-1}. In the cation, these modes are still strong, but are shifted to much higher frequencies (606.2 and 659.5 cm^{-1}). The removal of an electron from the π electron system apparently introduces some double bond character into the C−NH_2 bond making it more difficult to bend the hydrogens out of the plane. The out-of-plane bend for the quartet hydrogens occurs in 2-aminoanthracene cation at 756.4 cm^{-1} compared with 741.5 cm^{-1} in the neutral. This shift of 14.9 cm^{-1} can be compared to 11.5 cm^{-1} for 9-cyanoanthracene.

The matrix-isolation data for 2-aminoanthracene cation is in qualitative agreement with theory, although the lowest frequency that can unambiguously be ascribed to the cation occurs at 897.0 cm^{-1}. There are some notable differences in the relative intensities. For example, the experimental band at 1041.0 cm^{-1} is much stronger than our a′ harmonic at 1044.0 cm^{-1}. Also the two theoretical a′ harmonics at 1359.2 and 1383.0 cm^{-1} are much stronger than the three experimental bands observed between 1359.2 and 1379.2 cm^{-1}. Theory also obtains very strong bands at 1593.0 and 1658.0, which contain significant NH_2 in-plane bend character that are difficult to correlate with the four experimental bands in this spectral region—see Table 10. Theory and experiment agree on the N−H stretch mode being the strongest in 2-aminoanthracene. The agreement

TABLE 8: Infrared Frequencies and Relative Intensities for the 1-Methylanthracene Cation

	theory		experiment	
mode	frequency[a]	relative intensity[b]	frequency	relative intensity
1	84.3	0.004		
2	87.1	0.001		
3	121.2	0.004		
4	184.7	0.002		
5	234.3	0.001		
6	275.0	0.001		
7	315.7	0.002		
8	389.9	0.013		
9	439.7	0.001		
10	443.1	0.052		
11	510.3	0.001		
12	512.8	0.001		
13	536.8	0.002		
14	567.2	0.001		
15	617.6	0.003		
16	652.2	0.002		
17	705.0	0.006		
18	725.2	0.016		
19	745.0	0.015		
20	757.7	0.135		
21	781.7	0.014		
22	787.3	0.055		
23	847.0	0.001		
24	866.3	0.001		
25	907.5	0.056		
26	919.4	0.044	953.9	0.052
27	942.0	0.009		
28	968.2	0.002		
29	980.7	0.013		
30	1008.8	0.001		
31	1022.8	0.007		
32	1040.6	0.001		
33	1051.0	0.015		
34	1084.9	0.019		
35	1179.7	0.048	1186.9	0.203
36	1190.3	0.006		
37	1198.3	0.086		
38	1211.5	0.317	1210.6/1214.4	0.405
39	1250.3	0.077	1257.4	0.094
40	1276.8	0.015		
41	1285.3	0.067		
42	1293.7	0.004		
			1323.5	0.257
43	1333.4	1.000	1339.1	1.000
44	1364.0	0.046	1377.2	0.141
45	1380.2	0.303	1397.7/1396.5	0.271
46	1402.8	0.089	1414.4	0.044
47	1410.2	0.030	1418.9	0.390
48	1435.4	0.047	1431.4	0.074
49	1458.2	0.096	1463.4/1459.3	0.264
50	1471.2	0.048		
51	1478.5	0.105		
52	1484.3	0.031		
53	1507.0	0.018		
54	1523.1	0.197		
55	1528.2	0.095	1545.0/1539.1	0.213
56	1547.8	0.018		
57	1561.5	0.188	1583.5	0.144
58	2915.5	0.004		
59	2968.9	0.013		
60	3016.9	0.027		
61	3063.8	0.001		
62	3073.7	0.002		
63	3076.3	0.004		
64	3076.7	0.001		
65	3083.3	0.005		
66	3083.9	0.003		
67	3091.6	0.005		
68	3100.3	0.015		
69	3103.9	0.015		

[a] Theoretical frequencies (in cm^{-1}) are scaled by 0.958. [b] The absolute intensities (in km/mol) can be obtained by multiplying by the factor of 361.775.

TABLE 9: Infrared Frequencies and Relative Intensities for the 9-Methylanthracene Cation

	theory		experiment	
mode	frequency[a]	relative intensity[b]	frequency	relative intensity
1	29.1	0.003		
2	131.4	0.007		
3	243.4	0.001		
4	300.3	0.007		
5	388.6	0.007		
6	508.5	0.031		
7	510.9	0.001		
8	584.0	0.007		
9	608.3	0.002		
10	746.8	0.094	747.2	0.191
11	770.0	0.126	773.9	0.092
12	815.3	0.004		
13	854.2	0.004		
14	865.3	0.017		
15	904.1	0.007		
16	923.9	0.031		
17	979.9	0.008		
18	1019.9	0.039		
19	1027.5	0.005		
20	1030.0	0.001		
21	1035.5	0.001		
22	1074.9	0.042		
23	1101.4	0.013		
24	1203.7	0.100	1191.8	0.279
25	1254.6	0.027	1236.1	0.031
26	1260.3	0.010	1253.7	0.126
27	1294.2	0.013		
28	1311.1	0.103	1332.7/1334.9	0.289
29	1332.1	1.000	1343.4	1.000
			1353.0	0.849
30	1344.4	0.009		
31	1367.3	0.013		
32	1401.8	0.035	1408.8	0.251
33	1412.4	0.027	1411.6	0.053
34	1436.7	0.040		
35	1452.7	0.042		
36	1465.9	0.036		
37	1471.5	0.010		
38	1496.2	0.044		
39	1509.8	0.027		
40	1526.8	0.115	1542/1538.9	0.127
41	1534.5	0.002		
42	1545.0	0.006		
43	1567.3	0.128		
44	2922.1	0.001		
45	2971.4	0.003		
46	3062.6	0.014		
47	3075.2	0.002		
48	3075.6	0.002		
49	3086.7	0.002		
50	3087.8	0.001		
51	3101.0	0.006		
52	3102.4	0.007		
53	3111.2	0.008		
54	3120.6	0.010		

[a] Theoretical frequencies (in cm^{-1}) are scaled by 0.958. [b] The absolute intensities (in km/mol) can be obtained by multiplying by the factor of 465.350.

between theory and experiment is thus much less satisfactory for the cation than the corresponding neutral system.

The DFT frequencies and relative intensities for acridine are compared with the matrix isolation values in Table 11. Theory predicts two nearly equal, very intense b_2 harmonics at 1228.0 and 1311.4 cm^{-1}. Experiment is in complete accord with bands at 1217.1/1220.7 cm^{-1} and 1313.9/1316.8 cm^{-1}. The sum of the intensities of the three experimental bands at 1327.7, 1341.0, and 1357.1 cm^{-1} are comparable to the theoretical harmonic at

TABLE 10: Infrared Frequencies and Relative Intensities for the 2-Aminoanthracene Cation

	theory		experiment	
irreducible representation	frequency[a]	relative intensity[b]	frequency	relative intensity
a″	67.0	0.008		
a″	173.0	0.001		
a′	196.7	0.004		
a″	245.0	0.001		
a″	310.9	0.005		
a′	323.8	0.002		
a″	391.1	0.001		
a″	434.7	0.054		
a′	438.9	0.001		
a″	457.4	0.005		
a′	499.2	0.021		
a″	518.3	0.006		
a″	606.2	0.171		
a′	624.8	0.002		
a′	655.9	0.014		
a″	659.5	0.417		
a″	722.9	0.009		
a′	740.7	0.005		
a″	748.3	0.003		
a″	756.4	0.112		
a′	773.9	0.007		
a″	818.7	0.048		
a′	842.1	0.017		
a″	846.6	0.050		
a″	870.8	0.009		
a′	907.2	0.009		
a″	907.5	0.133	897.0	0.035
a″	928.0	0.022	917.0	0.009
a′	943.4	0.047	944.4	0.069
a″	975.8	0.011		
a″	988.4	0.001		
a′	1020.6	0.002		
a′	1044.0	0.016	1041.0	0.322
a′	1114.5	0.002		
a′	1157.3	0.025	1160.4	0.016
			1166.5	0.020
a′	1183.7	0.005	1183.6	0.079
a′	1193.7	0.152	1188.6	0.008
a′	1201.2	0.157		
a′	1230.5	0.007		
a′	1274.7	0.025	1274.3	0.027
a′	1288.9	0.037	1283.0	0.013
a′	1298.5	0.006		
a′	1346.1	0.426	1345.6	0.304
a′	1359.2	0.231	1359.2	0.037
			1366.0	0.044
a′	1383.0	0.281	1379.2	0.024
a′	1390.8	0.123		
a′	1409.5	0.022	1410.4	0.169
a′	1454.6	0.133	1425.8/1428.5	0.034
a′	1468.5	0.252	1463.7	0.194
a′	1491.7	0.022	1474.2	0.021
a′	1505.3	0.026		
a′	1527.6	0.126		
a′	1550.9	0.169		
a′	1560.0	0.002	1581.3	0.037
a′	1593.0	0.732	1636.1	0.391
a′	1658.0	0.500	1656.6	0.058
			1739.0	0.024
a′	3062.3	0.003		
a′	3064.4	0.001		
a′	3067.4	0.013		
a′	3071.3	0.001		
a′	3071.8	0.004		
a′	3074.5	0.001		
a′	3087.3	0.012		
a′	3088.7	0.008		
a′	3101.3	0.022		
a′	3428.2	1.000	3406.5	1.000
a′	3540.6	0.110		

[a] Theoretical frequencies (in cm^{-1}) are scaled by 0.958. [b] The absolute intensities (in km/mol) can be obtained by multiplying by the factor of 505.02.

TABLE 11: Infrared Frequencies and Relative Intensities for the Acridine Cation

	theory		experiment	
irreducible representation	frequency[a]	relative intensity[b]	frequency	relative intensity
b_1	88.0	0.014		
a_1	234.5	0.006		
b_1	265.6	0.011		
b_1	385.7	0.010		
b_2	403.3	0.003		
b_1	453.5	0.033		
b_2	509.7	0.001		
b_1	554.7	0.001		
b_2	598.0	0.046		
a_1	615.1	0.010		
a_1	657.3	0.004		
a_1	730.0	0.003		
b_1	751.0	0.261		
b_1	796.4	0.097		
b_2	809.4	0.088		
b_1	877.2	0.072		
a_1	895.3	0.005		
b_2	920.9	0.008		
b_1	947.0	0.027		
b_1	989.3	0.023		
b_2	1014.3	0.026		
b_2	1091.7	0.005		
b_2	1170.3	0.034		
a_1	1189.2	0.001		
b_2	1192.7	0.037		
b_2	1228.0	0.995	1217.1/1220.7	0.977
a_1	1240.9	0.001	1234.0/1236.1	0.168
a_1	1273.3	0.042		
a_1	1300.0	0.001		
b_2	1311.4	1.000	1313.9/1316.8	1.000
			1327.7	0.345
b_2	1342.1	0.597	1341.0	0.093
a_1	1369.4	0.009	1357.1	0.109
b_2	1391.6	0.044		
b_2	1423.4	0.066		
a_1	1456.7	0.134		
b_2	1465.4	0.099		
b_2	1505.9	0.185		
b_2	1522.7	0.183		
a_1	1530.1	0.003	1536.8	0.136
a_1	1565.2	0.214		
b_2	3075.1	0.004		
a_1	3075.4	0.001		
a_1	3091.6	0.005		
b_2	3101.7	0.005		
a_1	3101.9	0.001		
b_2	3111.3	0.015		
a_1	3111.5	0.005		

[a] Theoretical frequencies (in cm^{-1}) are scaled by 0.958. [b] The absolute intensities (in km/mol) can be obtained by multiplying by the factor of 307.48.

1342.1 cm^{-1}. There are several moderately strong harmonics between 1500 and 1565 cm^{-1} in the theoretical spectrum, but only one experimental band at 1536.8 cm^{-1} that can be ascribed to the cation. This is probably due to interference from the neutral system, which has many bands in this spectral region—see Table 6 and Figure 8. The out-of-plane C−H bend due to the quartet hydrogens occurs in acridine cation at 751.0 cm^{-1} compared with 742.8 cm^{-1} for the neutral. This shift is smaller than for either CN or NH_2 substitution on the ring. Although a significant fraction of the harmonics are not observed experimentally for acridine cation, the bands that are observed correspond reasonably well with theory.

5. Conclusions

We find that adding a methyl or cyano side group to anthracene or substituting nitrogen for one of the carbon ring atoms does not significantly alter the spectrum of either the neutral or positive ion, except to introduce the characteristic methyl or C≡N frequency and to spread the spectral intensity into more bands as a result of the reduced symmetry. In contrast, adding an NH_2 group dramatically affects both the neutral and cationic spectra. Besides adding the strong N−H stretch and bending modes, the NH_2 group withdraws charge from the ring, thereby giving the neutral aminoanthracene spectra many of the characteristics of cationic PAH spectra. We observe that the sum of the intensities of the harmonics in neutral 2-aminoanthracene to be four times that of unsubstituted anthracene.

The calculated harmonics for the substituted anthracenes considered in this work are in very good agreement with matrix-isolation studies for the neutral species, but are only in qualitative agreement for the cationic species. The matrix isolation experiments are more difficult for the cations because they must be measured against a strong background signal from the neutral species. In addition, there are potentially other molecular species present after photolysis. The DFT calculations are also subject to greater uncertainty for the open-shell cations, since the cations are not as well-described by a single reference configuration as are the neutrals. Thus, while theory offers a nearly unambiguous assignment of the matrix-isolation spectra of the neutrals, the assignments for the cations must be considered tentative. Nevertheless, theory combined with experiment shows that the spectra of substituted PAHs can be reliably determined. Thus, we feel confident that this study accurately depicts the effect of methyl, amino, and cyano substitution on the ring and nitrogen substitution in the ring.

References and Notes

(1) (a) Lee, M. L.; Novotny, M. V.; Bartle, K. D. *Analytical Chemistry of Polycyclic Aromatic Compounds*; Academic Press: New York, 1981; Chapter 2. (b) Yürüm, Y., Ed.; *New Trends in Coal Science*; NATO ASI Series, Series C: Mathematical and Physical Sciences 244; Kluwer Academic Publishers: Dordrecht, 1988.

(2) (a) Harris, S. J.; Weiner, A. M. *Combust. Sci. Technol.* **1983**, *31*, 155. (b) Frenklach, M.; Warnatz, J. *Combust. Sci. Technol.* **1987**, *51*, 265.

(3) Harvey, R. G., Ed. *Polycyclic Hydrocarbons and Carcinogenesis*; American Chemical Society: Washington, DC, 1985.

(4) (a) Duley, W. W.; Williams, D. A. *Mon. Not. R. Astron. Soc.* **1981**, *196*, 269. (b) Leger, A.; Puget, J. L. *Astron. Astrophys.* **1984**, *137*, L5. (c) Allamandola, L. J.; Tielens, A. G. G. M.; Barker, J. R. *Astrophys. J.* **1985**, *290*, L25.

(5) Allamandola, L. J.; Tielens, A. G. G. M.; Barker, J. R. *Astrophys. J. Suppl. Ser.* **1989**, *71*, 733.

(6) (a) DeFrees, D. J.; Miller, M. D. In *Interstellar Dust: Contributed Papers*; Allamandola, L. J., Tielens, A. G. G. M., Eds.; NASA Conference Proceeding CP-3036, National Aeronautics and Space Administration: Washington, DC, 1989; p 173. (b) Pauzat, F.; Talbi, D.; Miller, M. D.; DeFrees, D. J.; Ellinger, Y. *J. Phys. Chem.* **1992,** *96*, 7882. (c) Rougeau, N.; Flament, J. P.; Youkharibache, P.; Gervais, H. P.; Berthier, G. *J. Mol. Struct. (THEOCHEM)* **1992**, *254*, 405. (d) Talbi, D.; Pauzat, F.; Ellinger, Y. *Astron. Astrophys.* **1993**, *268*, 805. (e) Cebe, E.; Grampp, G. *Z. Phys. Chem.* **1994**, *187*, 15. (f) Martin, J. M. L. *Chem. Phys. Lett.* **1996**, *262*, 97. (g) Martin, J. M. L.; El-Yazal, J.; Francois, J.-P. *J. Phys. Chem.* **1996**, *100*, 15358. (h) Ho, Y.-P.; Yang, Y.-C.; Klippenstein, S. J.; Dunbar, R. C. *J. Phys. Chem.* **1995**, *99*, 12115.

(7) Bauschlicher, C. W.; Langhoff, S. R.; Sandford, S. A.; Hudgins, D. M. *J. Phys. Chem.* **1997**, *101*, 2414.

(8) Langhoff, S. R. *J. Phys. Chem.* **1996**, *100*, 2819.

(9) See: (a) Flickinger, G. C.; Wdowiak, T. J.; Gomez, P. L. *Astrophys. J.* **1991**, *380*, L43. (b) Semmler, J.; Yang, P. W.; Crawford, G. E. *Vib. Spectrosc.* **1991**, *2*, 189. (c) Brenner, J.; Barker, J. *Astrophys. J.* **1992**, *388*, L39. (d) Kurtz, J. *Astron. Astrophys.* **1992**, *255*, L1. (e) Schlemmer, S.; Cook, D. J.; Harrison, J. A.; Wurfel, B.; Chapman, W.; Saykally, R. J. *Science* **1994**, *265*, 1686. (f) Joblin, C.; Boissel, P.; Léger, A.; d'Hendecourt, L.; Defourneau, D. *Astron. Astrophys.* **1995**, *299*, 835 and references therein.

(10) Shan, J.; Suto, M.; Lee, L. C. *Astrophys. J.* **1991**, *383*, 459.

(11) Cook, D. J.; Schlemmer, S.; Balucani, N.; Wagner, D. R.; Steiner, B.; Saykally, R. J. *Nature* **1996**, *380*, 227.

(12) See: (a) Stout, P.; Mamantov, G. In *Chemical Analysis of Polycyclic Aromatic Compounds*; Vo-Dinh, T., Ed.;, John Wiley and Sons: New York, 1989, p 411. (b) Hudgins, D. M.; Allamandola, L. J. *J. Phys. Chem.* **1995**,

99, 8978. (c) Szczepanski, J.; Wehlburg, C.; Vala, M. *Chem. Phys. Lett.* **1995**, *232*, 221. (d) Szczepanski, J.; Drawdy, J.; Wehlburg, C.; Vala, M. *Chem. Phys. Lett.* **1995**, *245*, 539. (e) Bernstein, M. P.; Sandford, S. A., Allamandola, L. J. *Astrophys. J.* **1996**, *472*, L127. (f) Hudgins, D. M.; Allamandola, L. J. *J. Phys. Chem.* **1997**, *101*, 3472 and references therein.

(13) Hudgins, D. M.; Allamandola, L. J. *J. Phys. Chem.* **1995**, *99*, 3033.

(14) Joblin, C. 1992, Ph.D. Thesis, l'Université, Paris 7.

(15) Atkinson, R.; Arey, J.; Winer, A. M.; Zielinska, B.; Dinoff, T. M.; Harger, W. P.; McElroy, P. A. In A Survey of Ambient Concentrations of Selected Polycyclic Aromatic Hydrocarbons (PAH) at Various Locations in California. Final Report, Contract No. A5-185-32; California Air Resources Board, Statewide Air Polluiton Research Center, University of California at Riverside; Riverside, 1988; p IX-1.

(16) cf. Hecht, S. S.; Amin, S.; Melikian, A. A.; LaVoie, E. J.; Hoffmann, D. In *Polycyclic Hydrocarbons and Carcinogenesis*; Harvey, R. G., Ed.; American Chemical Society: Washington, DC, 1985; p 85.

(17) cf. Marnett, L. J. In *Polycyclic Hydrocarbons and Carcinogenesis*; Harvey, R. G.; Ed.; American Chemical Society: Washington, DC, 1985; p 307.

(18) cf. Beland, F. A.; Heflich, R. H.; Howard, P. C.; Fu, F. P. In *Polycyclic Hydrocarbons and Carcinogenesis*; Harvey, R. G., Ed.; American Chemical Society: Washington, DC, 1985; p 371.

(19) cf. Mullie, F.; Reisse, J. *Top. Curr. Chem.* **1987**, *139*, 83.

(20) Kerridge, J. F.; Chang, S.; Shipp, R. *Geochim. Cosmochim. Acta* **1987**, *51*, 2527.

(21) (a) Sandford, S. A. *Fundamentals of Cosmic Physics* **1987**, *12*, 1. (b) Allamandola, L. J.; Sandford, S. A.; Wopenka, B. *Science* **1987**, *237*, 56. (c) Bradley, J. P.; Sandford, S. A.; Walker, R. M. In *Meteorites and the Early Solar System*; Kerridge, J. F., Matthews, M. S., Eds.; University Arizona Press: Tucson, 1988; p 861.

(22) Clemett, S.; Maechling, C.; Zare, R. N.; Swan, P.; Walker, R. *Science* **1993**, *262*, 721.

(23) cf. (a) Studier, M. H.; Hayatsu, R.; Anders, E. *Geochim. Cosmochim. Acta* **1972**, *36*, 189. (b) Tingle, T. N.; Becker, C. H.; Malhotra, R. *Meteoritics* **1991**, *26*, 117. (c) Kovalenko, L. J.; Maechling, C. R.; Clemett, S. J.; Philippoz, J. M.; Zare, R. N.; Alexander, C. M. O'D. *Anal. Chem.* **1992**, *64*, 682.

(24) cf. Geballe, T. R.; Tielens, A. G. G. M.; Allamandola, L. J.; Moorhouse, A.; Brand, P. W. J. L. *Astrophys. J.* **1989**, *341*, 278.

(25) Bauschlicher, C. W.; Langhoff, S. R. *Mol. Phys.* **1998**. Submitted for publication.

(26) Stephens, P. J.; Devlin, F. J.; Chabalowski, C. F.; Frisch, M. J. *J. Phys. Chem.* **1994**, *98*, 11623.

(27) Becke, A. D. *J. Chem. Phys.* **1993,** *98*, 5648.

(28) Frisch, M. J.; Trucks, G. W.; Schlegel, H. B.; Gill, P. M. W.; Johnson, B. G.; Robb, M. A.; Cheeseman, J. R.; Keith, T.; Petersson, G. A.; Montgomery, J. A.; Raghavachari, K.; Al-Laham, M. A.; Zakrzewski, V. G.; Ortiz, J. V.; Foresman, J. B.; Cioslowski, J.; Stefanov, B. B.; Nanayakkara, A.; Challacombe, M.; Peng, C. Y.; Ayala, P. Y.; Chen, W.; Wong, M. W.; Andres, J. L.; Replogle, E. S.; Gomperts, R.; Martin, R. L.; Fox, D. J.; Binkley, J. S.; Defrees, D. J.; Baker, J.; Stewart, J. P.; Head-Gordon, M.; Gonzalez, C.; Pople, J. A. GAUSSIAN 94, Revision D.1; GAUSSIAN, Inc.: Pittsburgh, PA, 1995.

(29) Frisch, M. J.; Pople, J. A.; Binkley, J. S. *J. Chem. Phys.* **1984**, *80*, 3265 and references therein.

(30) Bauschlicher, C. W. Langhoff, S. R. *Spectrochim. Acta A* **1997**, *53*, 1225.

(31) Hudgins, D. M.; Sandford, S. A. *J. Phys. Chem.* **1998**, *102*, 329; **1998**, *102*, 344; **1998**, *102*, 353.

(32) Hudgins, D. M.; Sandford, S. A.; Allamandola, L. J. *J. Phys. Chem.* **1994**, *98*, 4243.